

MAJOR ARTICLE

Resistance to Oxidative Stress Is Associated with Metastasis in Mucocutaneous Leishmaniasis

Nathalie Acestor,^{1,a} Slavica Masina,¹ Annette Ives,¹ John Walker,² Nancy G. Saravia,² and Nicolas Fasel¹

¹Department of Biochemistry, University of Lausanne, Epalinges, Switzerland; ²Centro Internacional de Entrenamiento e Investigaciones Médicas, Cali, Colombia

Mucocutaneous leishmaniasis (MCL) in South and Central America is characterized by the dissemination (metastasis) of *Leishmania Viannia* subgenus parasites from a cutaneous lesion to nasopharyngeal tissues. Little is known about the pathogenesis of MCL, especially with regard to the virulence of the parasites and the process of metastatic dissemination. We previously examined the functional relationship between cytoplasmic peroxiredoxin and metastatic phenotype using highly, infrequently, and nonmetastatic clones isolated from an *L. (V.) guyanensis* strain previously shown to be highly metastatic in golden hamsters. Distinct forms of cytoplasmic peroxiredoxin were identified and found to be associated with the metastatic phenotype. We report here that peroxidase activity in the presence of hydrogen peroxide and infectivity differs between metastatic and nonmetastatic *L. (V.) guyanensis* clones. After hydrogen peroxide treatment or heat shock, peroxiredoxin was detected preferentially as dimers in metastatic *L. (V.) guyanensis* clones and in *L. (V.) panamensis* strains from patients with MCL, compared with nonmetastatic parasites. These data provide evidence that resistance to the first microbicidal response of the host cell by *Leishmania* promastigotes is linked to peroxiredoxin conformation and may be relevant to intracellular survival and persistence, which are prerequisites for the development of metastatic disease.

Mucocutaneous leishmaniasis (MCL) caused by *Leishmania Viannia* subgenus is one of the most severe forms of human tegumentary leishmaniasis. It produces a wide variety of symptoms—such as nasal congestion, deformities, malnutrition, and respiratory obstruction—and, in some cases, it leads to death [1]. This disease has been a challenge for clinicians and researchers because it is uncommon and its pathogenesis is poorly understood. In MCL, after the apparent cure of the primary lesion, secondary lesions may appear in the nasopharyngeal tissues of the infected host, which

is caused by the dissemination of the infection from the inoculation site [2, 3]. Both nasal and oral lesions are characterized by a severe inflammatory reaction. These sites are evidently colonized by the dissemination of infected macrophages via hematogenous and lymphatic routes in humans [4, 5] and in the golden hamster model [6, 7]. New lesions can appear several years after healing of the original cutaneous lesion, which may be triggered by trauma or inflammatory stimuli [3, 8]. The dissemination and consequent metastatic lesions lead to the disfiguring morbidity associated with MCL. The spectrum of the biological outcome of infection is influenced not only by the host immune status but also by differences in parasite virulence [6, 9, 10].

Previous work established heterogeneity among strains of *L. (V.) panamensis* and *L. (V.) guyanensis* with respect to their capacities to disseminate and to generate secondary metastatic lesions in the golden hamster model [6]. The subsequent isolation and characterization of several clones derived from a strain of *L. (V.) guyanensis* WHI/BR/78/M5313, which is highly

Received 27 February 2006; accepted 26 May 2006; electronically published 8 September 2006.

Financial support: Swiss National Science Foundation (grants 3170-059520.99 [for Research Partnership with Developing Countries to N.F.] and 3100-103813).

Potential conflicts of interest: none reported.

^a Present affiliation: Seattle Biomedical Research Institute, Seattle, Washington.

Reprints or correspondence: Prof. Nicolas Fasel, Dept. of Biochemistry, Faculty of Biology and Medicine, Ch. des Boveresses 155, CH-1066 Epalinges, Switzerland (Nicolas.Fasel@unil.ch).

The Journal of Infectious Diseases 2006;194:1160–7

© 2006 by the Infectious Diseases Society of America. All rights reserved.
0022-1899/2006/19408-0018\$15.00

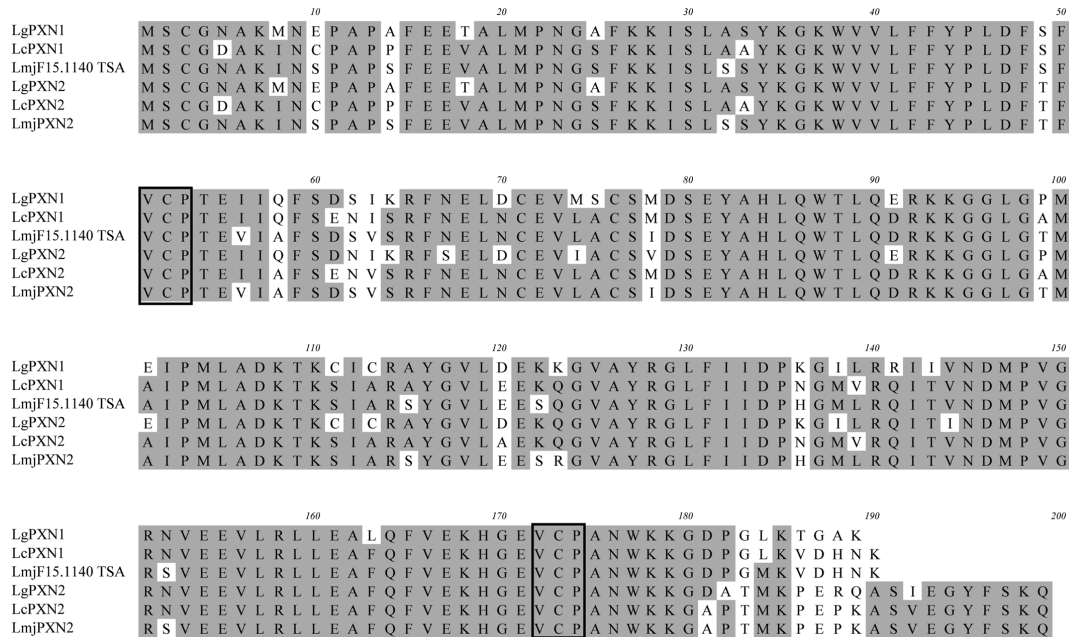


Figure 1. Sequence alignment of *Leishmania* peroxiredoxins (PXNs). Sequences in boxes indicate the 2 conserved valine-cysteine-proline (VCP) catalytic domains. Homologous regions are shaded in gray. GenBank accession nos. are as follows: LgPXN1, AY921646; LgPXN2, AY753537; LcPXN1 (*L. chagasi* PXN1), AF134161; LcPXN2 (*L. chagasi* PXN2), AF312397; LmjPXN2 (*L. major* PXN2), AF069386 and AF044679; LmjF15.1140TSA, GeneDB, contig: LmjF15_01_20040630_V4.0.

metastatic in the hamster, revealed stable interclonal phenotypic differences. Although all of the derived clones induced primary cutaneous lesions, some disseminated from the initial lesion and exhibited different phenotypes in hamsters, which allowed the classification of clones into 2 groups: metastatic (M^+) and nonmetastatic (M^-) [11]. Thus, the reproducible expression of metastasis by discrete populations of *Leishmania* parasites in golden hamsters provided an experimental model for the identification of factors involved in the metastatic process.

Recently, we used M^+ and M^- clones (together with clinical isolates of *L. Viannia* species from mucocutaneous or cutaneous lesions) as tools for the identification of gene products associated with metastasis in *Leishmania* species from South and Central America [12]. Comparative proteome analyses using 2-dimensional electrophoresis (2-DE) coupled with peptide fingerprinting, mass spectrometry (MS), and bioinformatics enabled the identification of differentially expressed proteins, including the cytoplasmic trypanosomatid peroxiredoxin (PXN), or tryparedoxin peroxidase. The association between phenotype and the differential expression of this protein was conserved in some but not all *L. Viannia* isolates from patients with MCL or cutaneous leishmaniasis [12].

Among trypanosomatids, PXN belongs to the 2-cysteine peroxiredoxin family (2-Cys PXN) and functions as the terminal peroxidase of a redox cascade that reduces hydroperoxides by NADPH [13–19]. 2-Cys PXNs require dimerization to exert

their protective antioxidant role in cells through their peroxidase activity, whereby hydrogen peroxide (H_2O_2), peroxinitrite, and a wide range of organic hydroperoxides are reduced and detoxified [20]. Detoxification is necessary as a defense process against reactive oxygen intermediates such as H_2O_2 , which are produced within 30 min of phagocytosis, and it therefore has essential protective functions for the infecting promastigote-stage parasite. Detoxification is also necessary later on for survival of the intracellular stage (the amastigote), when reactive nitrogen intermediate species such as nitric oxide (NO) are produced after the activation of macrophages by the host immune system [21, 22]. Thus, PXN could play an important role in the initial stage of infection and in the survival of the parasite when it enters the macrophage as a promastigote and differentiates into an intracellular amastigote.

In the present work, we analyzed the resistance to reactive oxygen species (ROS) of *L. (V.) guyanensis* clones and *L. (V.) panamensis* strains presenting disparate metastatic phenotypes. We characterized PXN at the DNA, protein, and enzymatic activity level, because it has been shown elsewhere to be present as different isoforms in M^+ and M^- parasites [12]. We demonstrate that PXN may be implicated in resistance to ROS and in the metastatic process of *L. Viannia* parasites. For a detailed description of the materials and methods used, see the Appendix, which is available at the *Journal's* Web site (<http://www.journals.uchicago.edu/JID/journal/home.html>).

RESULTS

Characterization of *L. (V.) guyanensis* Pxn genes. Molecular characterization of the *Pxn* gene(s) at the DNA level allowed us to determine whether the isoforms that had been detected previously by 2-DE in M^+ and M^- parasites [12] were simply due to polymorphisms in the allelic forms of the gene(s). A partial nucleotide sequence including the *Pxn* open reading frame was previously obtained on the basis of the initial sequence of tryptic fragments [12]. From this information, a reverse-transcription polymerase chain reaction (PCR) strategy was used to amplify a full-length sequence of *Pxn* in the M^+ clone 13 and the M^- clone 17. Two different copies of *Pxn* cDNA (*LgPxn1* and *LgPxn2*) were identified. *LgPxn1* and *LgPxn2* harbor identical sequences in M^+ and M^- clones, respectively, of *L. (V.) guyanensis*. The coding regions of *LgPxn1* and *LgPxn2* have a size of 570 and 600 nt, respectively. *LgPxn1* and *LgPxn2* were predicted to encode mature proteins of 21.2 and 22.5 kDa, with a theoretical isoelectric point (pI) of 8.14 and 6.19, respectively. Both copies encode members of the 2-Cys PXN, which are characterized by 2 highly conserved redox active-cysteine residues: the peroxidatic cysteine (Cys52) and the resolving cysteine (Cys173) present in the valine-cysteine-proline catalytic domains. An overall comparison of the LgPXN1 amino acid sequence with the LgPXN2 sequence for the predicted mature protein yielded an identity of 80% (figure 1). The 2 PXN sequences share a high degree of similarity with other PXNs from diverse *Leishmania* species [13, 15–19]. Two groups of PXN sequences can be distinguished according to their carboxyl terminus. The first group is shorter and consists of LgPXN1, LcPXN1, and LmjPXN1, whereas the second group consists of the longer PXNs belonging to LgPXN2, LcPXN2, and the *L. major* thiol-specific antioxidant protein (LmjF15.1140TSA). In yeast, this C-terminal extension has been shown to be important for the regulation of PXN activity [23].

This means that there are 2 copies of PXN in *L. (V.) guyanensis* that share sequence homology with PXNs in other *Leishmania* species [13]. These copies do not differ in sequence between M^+ and M^- parasites, which therefore excludes the possibility that the differences in PXN activity observed between the M^+ and M^- phenotypes are at the primary amino acid sequence level.

Analysis of LgPXN expression in promastigotes. Logarithmic to stationary-phase parasite extracts were separated on a 12% polyacrylamide gel under reducing and denaturing conditions. Immunoblot analysis was performed using a specific anti-LgPXN2 antibody. In stationary-phase M^- and M^+ promastigotes (figure 2A), the anti-LgPXN2 antibody clearly detected 2 immunoreactive bands at ~22 kDa, which correlates with the predicted molecular masses of 21.2 and 22.5 kDa for the LgPXN1 and LgPXN2 isoforms, respectively. Given that the protein patterns of PXN under reducing and denaturing con-

ditions did not differ between M^- and M^+ parasites and that PXNs are known to exist predominantly as active dimers in many organisms [24], the expression of PXN was further investigated in nonreducing electrophoretic mobility assays. In figure 2B, a diffuse band of ~45 kDa corresponding to oxidized dimers of PXN and lower bands of ~22 kDa corresponding to reduced monomers of PXN were seen throughout the life cycle of M^- promastigote parasites (figure 2B, lanes 1–3). By contrast, for the M^+ clone, the monomeric form of PXN was detected in logarithmic-phase parasites (figure 2B, lanes 4 and 5) but was barely detectable in stationary-phase parasites, where mostly the 45-kDa dimer was detected (figure 2B, lane 6). The

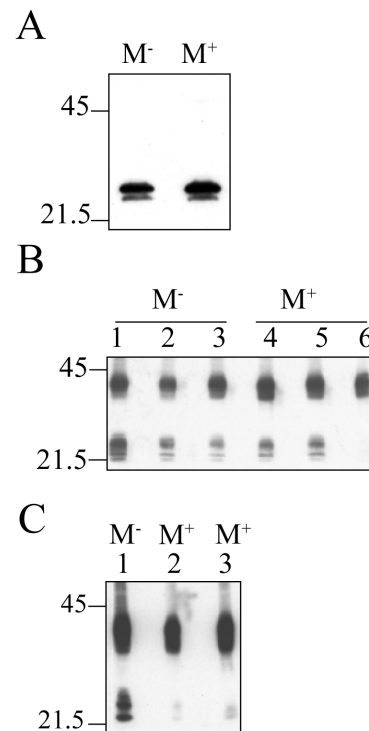


Figure 2. Comparison of peroxiredoxins (PXN) protein patterns between nonmetastatic (M^-) and metastatic (M^+) laboratory clones with a *Leishmania* isolate from a patient with mucocutaneous leishmaniasis. In total, 20 μ g of protein from M^- clone 17 and M^+ clone 13 parasites was extracted and resuspended in sample buffer with or without reducing agents. Proteins were size fractionated on a 12% polyacrylamide gel and transferred to a nitrocellulose membrane. Immunoblot was performed using a mouse polyclonal antibody against purified recombinant LgPXN2. Low-range molecular standards (in kilodaltons) (BioRad) were used. *A*, Total protein extracts from stationary-phase M^- or M^+ parasites resuspended in sample buffer that contained 100 mmol/L dithiothreitol and 0.2 mmol/L iodoacetamide. *B*, Total protein extracts from logarithmic-phase (lanes 1 and 4), late logarithmic-phase (lanes 2 and 5), and stationary-phase (lanes 3 and 6) M^- and M^+ parasites resuspended in sample buffer without reducing agents. *C*, Total protein extracts from M^- (lane 1), M^+ (lane 2), and human isolate 3008 *L. panamensis* M^+ (lane 3) stationary-phase parasites resuspended in sample buffer without reducing agents.

appearance of dimers in stationary-phase parasites from the M⁺ clone corroborated with the dimeric pattern observed in parasites isolated from a patient with MCL (figure e 2C, lanes 2 and 3). These results indicate that, under nonreducing conditions, the migration patterns of PXN differ between M⁻ and M⁺ stationary-phase parasites at a stage that is enriched in virulent parasites [25] and that more closely resembles those parasites found in clinical phenotypes.

Susceptibility of M⁺ and M⁻ promastigotes to H₂O₂-mediated toxicity. To investigate the expression of PXN during oxidative stress, promastigote parasites from 3 independent M⁺ and 2 independent M⁻ clones were exposed to varying concentrations of H₂O₂ (figure e 3). Immunodetection revealed the presence of monomers and dimers and the accumulation of PXN monomers in M⁻ parasites when they were exposed to >50 μmol/L H₂O₂ (figure e 3A and 3B). PXN was not shown to be present as a dimer alone under these conditions. In M⁺ parasites (figure e 3C, 3D, and 3E), monomeric forms of PXN were detected in the absence of H₂O₂ and then when the H₂O₂ concentration was increased to at least 250 μmol/L (figure e 3C, 3D, and 3E). To confirm this result, *L. (V.) panamensis* parasites isolated from human patients with MCL and that had been previously tested for their metastatic behavior in the golden hamster model (J.W., unpublished results) were exposed to

different concentrations of H₂O₂. In contrast to parasites from the nonmetastatic strain 2017 (figure e 4A), exposure to increasing concentrations of H₂O₂ (up to 1 mmol/L) did not alter the dimeric conformational state of PXN from the M⁺ strain 3008 (figure e 4B), with only a slight shift to monomeric form observed at 1 mmol/L H₂O₂. This confirmed the result obtained with the *L. (V.) guyanensis* M⁺ laboratory clones (figure e 3). In total, we analyzed 3 M⁻ and 4 M⁺ clones, including 2 clinical strains from 2 different *Leishmania* species. Our results demonstrate the ability of the PXN enzyme to form stable dimers in the presence of H₂O₂. The dimeric pattern of PXN differs between M⁺ and M⁻ parasites, likely because the presence of catalytically active cysteine residues in the M⁺ parasites renders them less susceptible to overoxidation by H₂O₂.

Peroxidase activity in promastigotes. The oxidation of NADPH was measured in the presence of 50 μmol/L H₂O₂ in promastigote extracts of M⁺ clone 13 and M⁻ clone 17 to determine peroxidase activity. Under these conditions, a peroxidase activity of 6.48 ± 0.78 μmol/min/L was detected in M⁻ parasite extracts, whereas a significantly higher level (*P* < .01)—10.21 ± 0.78 μmol/min/L—was found in M⁺ parasite extracts (table 1). Immunoblot analysis was performed to determine the subunit conformation of PXN before the addition of 50 μmol/L H₂O₂, in the presence of 50 μmol/L H₂O₂, and at the

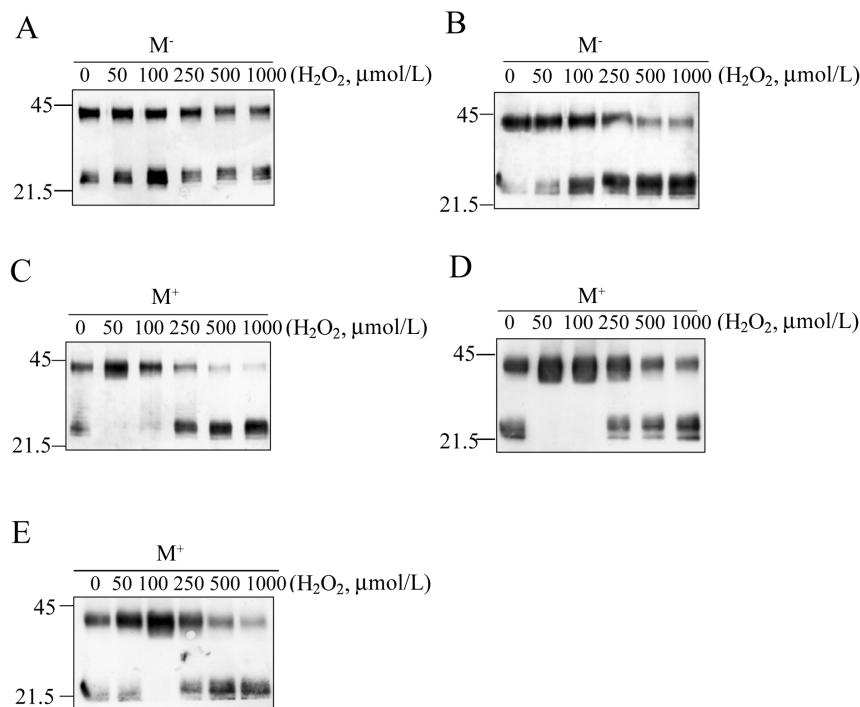


Figure 3. Alterations in the electrophoretic mobility of peroxiredoxin in nonmetastatic (M⁻) and metastatic (M⁺) laboratory clones after exposure to H₂O₂. A and B, Clones 3 and 17 M⁻ parasites, respectively. C, D, and E, Clones 13, 19, and 20 M⁺ parasites, respectively. For each sample, 20 μg of total protein was extracted from late logarithmic-phase parasites previously exposed to the indicated concentrations of H₂O₂ and resuspended in sample buffer without reducing agents. Immunoblotting was performed as described in the figure 2 legend. Low-range molecular standards (in kilodaltons) (BioRad) were used.

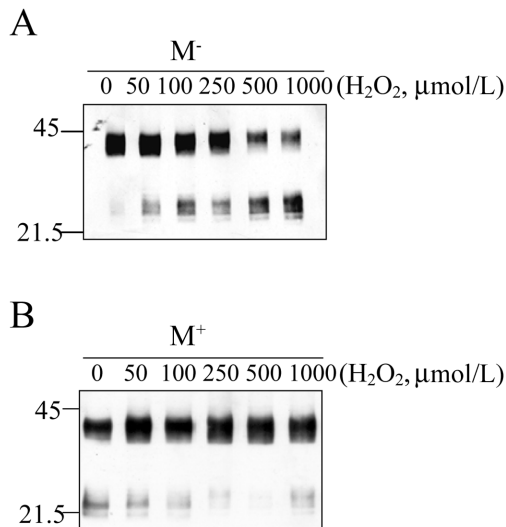


Figure 4. Electrophoretic mobility of peroxiredoxin in *Leishmania (Vivax) panamensis* human strains after exposure to H_2O_2 . *A*, Strain 2017 nonmetastatic (M^-) parasites. *B*, Strain 3008 metastatic (M^+) parasites. For panels *A* and *B*, 20 μg of total protein was extracted from late logarithmic-phase parasites previously exposed to the indicated concentrations of H_2O_2 and resuspended in sample buffer without reducing agents. Immunoblotting was performed as described in the figure 2 legend. Low-range molecular standards (in kilodaltons) (BioRad) were used.

end of the assay. This analysis revealed that M^- and M^+ PXN had a similar pattern before the addition of 50 $\mu mol/L$ H_2O_2 (figure 5, lanes 1 and 4). However, in the presence of 50 $\mu mol/L$ H_2O_2 and at the end of the assay, extracts from M^- parasites had both dimeric and monomeric forms of PXN present (figure 5, lanes 2 and 3), whereas, in M^+ extracts, only the 45-kDa dimer was detected (figure 5, lanes 5 and 6). These results show that, in M^+ promastigote extracts, peroxidase activity is higher than that in M^- parasite extracts, which corroborates the fact that M^+ and M^- parasites differ in their capability to form the stable PXN disulfid linkages necessary for the formation of a functional dimer.

Analysis of PXN conformation. To test whether M^+ and M^- *Leishmania* promastigotes harboring similar amounts of PXN monomeric and dimeric forms undergo conformational changes under stress, the parasites were exposed to a 37°C heat shock for 2 h (figure 6A and 6B). As shown in figure 6A, monomeric and dimeric forms present in the M^+ clone were shifted to only dimeric and high-molecular-weight complexes after heat shock (figure 6A, lane 4). Such a change in PXN conformation was not detected in M^- parasites (figure 6A, lane 2). This result provides additional evidence that M^+ and M^- parasites can be distinguished by their PXN conformation in a stress response situation, such as the change in temperature that the parasites would encounter in the macrophage environment.

Considering that metastasis is visible in long-term chronic

infections, it would be important to analyze whether the PXN pattern and activity differ between M^+ and M^- amastigotes. To answer this question, total protein was extracted from M^- amastigotes isolated from U937-infected cells (figure 6C, lane 1) and from M^+ and M^- axenic amastigotes grown at 34°C (figure 6C, lanes 2 and 3, respectively). Only the dimeric form of PXN could be detected in amastigotes and axenic M^+ and M^- parasites. To confirm that this dimeric conformation correlated with peroxidase activity, we measured the oxidation of NADPH in the presence of 500 $\mu mol/L$ H_2O_2 in axenic amastigote extracts of M^+ clone 13 and M^- clone 17. Preliminary results demonstrated that, during the amastigote-like stage, both clones have similar peroxidase activity (data not shown), which provides additional evidence that the dimeric PXN conformation pattern likely corresponds to a high degradation activity of ROS.

These results prompted us to test the survival of promastigotes at 37°C in the presence of H_2O_2 , thus mimicking the stress situation encountered by the parasite after the first hours of infection (figure 6D). After a 2-h incubation at 37°C, we observed, using the MTS assay (CellTiter96; Promega), an increased survival of M^+ compared with M^- parasites. Furthermore, M^+ parasites were more resistant to H_2O_2 than were M^- parasites up to a concentration of 0.5 mmol/L. These results confirmed the direct relationship between the formation of PXN dimers and resistance to oxidative stress in conditions mimicking the situation encountered by infectious promastigotes entering mammalian host macrophages.

Virulence of M^+ and M^- parasites. Virulent versus avirulent strains of *L. donovani* have been shown to have significant differences in terms of their levels of resistance to H_2O_2 [26]. Therefore, we analyzed the virulence of M^+ clone 13 and M^- clone 17 parasites using an in vitro infection assay. As shown in table 2, the rate of infectivity and the parasite load were higher in bone marrow-derived macrophages infected with M^+ parasites than in M^- parasites. It has previously been shown that *Leishmania* parasites up-regulate NO production by murine macrophages [21, 27, 28]. In our hands, an enhancement of NO production was observed in macrophages harboring M^+ parasites after their stimulation with recombinant murine in-

Table 1. Peroxidase activity measured via the oxidation of NADPH.

Clone	Units of activity, $\mu mol/min/L$ of NADPH consumption
M^- clone 17	6.48 \pm 0.78
M^+ clone 13	10.21 \pm 0.78

NOTE. Peroxidase activity was measured via the oxidation of NADPH in the presence of 50 $\mu mol/L$ H_2O_2 . Data are the mean \pm SD of 3 experiments. M^+ , metastatic clone; M^- , nonmetastatic clone.

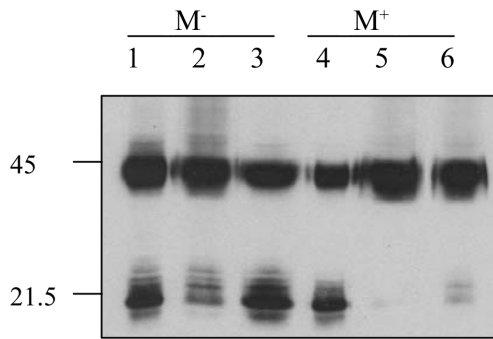


Figure 5. Pattern of peroxiredoxin protein expression during H_2O_2 detoxification. A total of 20 μg of cell lysates from clone 17 nonmetastatic (M^-) (lanes 1–3), or clone 13 metastatic (M^+) (lanes 4–6) late logarithmic-phase promastigotes was resuspended in sample buffer without reducing agents. Untreated parasite lysates (lanes 1 and 4), 50 $\mu\text{mol/L}$ H_2O_2 -treated parasite lysates (lanes 2 and 5), and lysates of parasites taken at the end of the enzymatic assay (lanes 3 and 6) are shown. Immunoblotting was performed as described in the figure 2 legend. Low-range molecular standards (in kilodaltons) (BioRad) were used.

terferon (IFN)- γ and lipopolysaccharide (LPS), relative to macrophages infected with M^- parasites (table 2). This latter result relates to the increase in parasite load observed for M^+ parasites and supports the notion that M^+ parasites were more efficiently phagocytosed by the macrophage than were M^- parasites and further supports there being a difference between M^+ and M^- parasite behavior during the first hours of infection. The parasite load was also compared at different time points after infection. More parasites could be detected in some experiments after 4 h of infection with M^- parasites; however, the rate of infection was always lower for M^- than for M^+ parasites after 24 h of infection (data not shown). Thus, although an enhancement of NO production was observed in macrophages infected by M^+ parasites, they nevertheless survived better than M^- parasites in the host macrophages.

DISCUSSION

In the present article, we describe the presence of 2 cytoplasmic PXN copies of *L. (V.) guyanensis*. This is in agreement with previous reports of other *Leishmania* PXNs [13, 15–19]. Furthermore, the level of expression of these copies was similar between M^+ and M^- parasites, which provides strong evidence that differences in PXN posttranslational modification or in the PXN protein conformation may be important in peroxidase activity, survival, and the distinct metastatic behavior of *L. guyanensis* parasites.

Dimerization of the 2-Cys PXN is required for the detoxification of H_2O_2 [29]. We have demonstrated, using an enzymatic assay measuring the oxidation of NADPH, that the reduction of H_2O_2 in vitro differs between M^+ and M^- pro-

mastigote parasites. In M^+ promastigotes, detoxification activity was significantly higher than that in M^- parasites, which correlates with PXN proteins being more prone to form active stable dimers than M^- promastigotes when they are treated with increasing concentrations of H_2O_2 . The expression of PXN mainly as a dimer in stationary M^+ promastigotes (figure 2), together with their relative resistance to H_2O_2 toxicity, correlates with the results of a previous study in which stationary-phase promastigotes were less susceptible to H_2O_2 than logarithmic-phase promastigotes [30]. In a metastatic *L. (V.) panamensis* clinical isolate, PXN also forms stable dimers in the absence or at the time of H_2O_2 exposure, as evidenced under non-reducing conditions. Moreover, these findings are in agreement with our previous observations, in which the expression profile

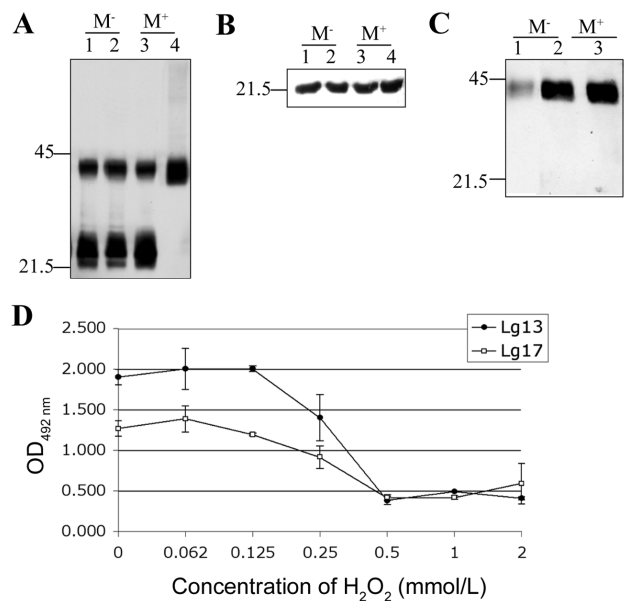


Figure 6. Peroxiredoxin conformation in nonmetastatic (M^-) and metastatic (M^+) clones after heat-shock treatment. *A* and *B*, Promastigotes of M^- clone 17 (lanes 1 and 2) or M^+ clone 13 (lanes 3 and 4) parasites were incubated at room temperature (lanes 1 and 3) or at 37°C for 2 h (lanes 2 and 4) under nonreducing (*A*) or reducing (*B*) conditions, to confirm equal loading of the samples. *C*, Amastigotes of M^- clone 17 parasites in U937-infected cells (lane 1), axenic amastigotes of M^- clone 17 parasites (lane 2), and axenic amastigotes of M^+ clone 13 parasites (lane 3). Immunoblotting was performed as described in the figure 2 legend. For panels *A*, *B*, and *C*, 20 μg of total protein was extracted and resuspended in sample buffer with (*B*) or without (*A* and *C*) reducing agents. Low-range molecular standards (in kilodaltons) (BioRad) were used. *D*, Measurement of cell viability at 37°C in the presence of different concentrations of H_2O_2 . A total of 2×10^6 promastigotes of M^- clone 17 or M^+ clone 13 parasites was incubated at 37°C for 2 h, followed by incubation for 1 h in the presence of different concentrations of H_2O_2 . The reaction was stopped by addition of 10% fetal calf serum and 500 U of catalase. Viability was measured using the MTS reagent (CellTiter 96; Promega). Absorbance was read at 492 nm.

Table 2. Infectivity of nonmetastatic (M⁻) and metastatic (M⁺) clones and nitric oxide (NO) production in bone marrow-derived macrophages.

Clone	Infectivity, %	Parasites/ macrophages, no.	NO ₂ ⁻ , μmol/L ^a
M ⁻	85	4	48.83 ± 2.61
M ⁺	98	8	65.59 ± 2.74

^a Macrophages infected with M⁻ or M⁺ parasites were stimulated with interferon-γ (50 U/mL) plus lipopolysaccharide (10 ng/mL), and NO production was measured as the rate of NO₂⁻ release in 48-h supernatants, as determined using the Griess reaction [27]. Data are the mean ± SD of 3 assays.

of PXN isoforms were associated with the highly, infrequently, or nonmetastatic phenotype of *L. (V.) guyanensis* laboratory clones and in some *L. (V.) panamensis* clinical strains [12].

At the molecular level, the increased susceptibility to monomer formation in M⁻ parasites is likely due to the selective overoxidation of the active-site cysteine (Cys52) in PXN to cysteine sulfinic acid (Cys-SO₂H) during catalysis. As has been shown in other cases [31], oxidation of the active-site cysteines of PXN caused by oxidative stress results in a shift in the pI to generate acidic protein variants. Such modification could also influence the formation of dimers. We previously reported a difference in pI for PXN in M⁺ and M⁻ parasites as determined using 2-DE and MS [12]. By using 2-DE and immunodetection with a specific anti-LgPXN2 antibody, we have preliminary evidence to suggest that pIs of PXN isoforms in M⁺ and M⁻ parasites differ when they are exposed to different concentrations of H₂O₂. These shifts in pI may be due to differences in the oxidative state of PXN and may explain the different conformations and susceptibility to H₂O₂ that we observed in the present study. We have also previously shown that not only PXN but also several proteins differ in their pIs in M⁺ and M⁻ parasites [12]. These data support the hypothesis of a general difference in the redox status in M⁺ and M⁻ parasites. Recently, protein glutathionylation has been proposed as a possible redox regulation of protein functions. Disulfide bridges can be formed between glutathione and the cysteine of proteins like PXN [32]. A similar posttranslational modification by trypanothione could affect the formation of dimers in trypanosomatids and, thus, regulate the different peroxidase activity detected in M⁺ and M⁻ parasites. The relevance of such a posttranslational mechanism can now be further explored.

Taken together, these results suggest that dimerization is linked with the functional activity of PXN in relation with the metastatic phenotype. Furthermore, we demonstrated, in an in vitro infection assay, that M⁺ parasites had a higher rate of infection in bone marrow-derived macrophages. After the activation of macrophages by IFN-γ and LPS, M⁺ parasites had greater resistance to oxidative stress as measured by NO pro-

duction and intracellular parasite survival. This resistance to oxidative stress is an important factor in explaining the increased virulence of M⁺ parasites entering host cells, considering that it is at this stage when parasites will encounter the oxygen burst produced during phagocytosis.

In *L. chagasi*, resistance to oxidative stress was shown to be induced by a 37°C heat shock [33]—this corresponds to the temperature encountered by the promastigote parasite when it is introduced in mammalian skin by the sand fly vector. Our data suggest that stress, such as an increase in temperature and the presence of H₂O₂, could favor the presence of active dimeric and multimeric forms of PXN in M⁺ parasites. Under these conditions, we observed that M⁺ parasites survive better than M⁻ parasites. Similarly, oxidative stress and heat-shock exposure of yeast cells causes the protein structures of PXN to shift from low-molecular-weight species to high-molecular-weight complexes [34]. This, in turn, triggers a peroxidase-to-chaperone functional switch. The chaperone function of these proteins enhances yeast resistance to heat shock.

Although we have not formally demonstrated that the dimerization of PXN is responsible for increased detoxification in M⁺ parasites, we provide strong evidence that dimer formation of PXN in M⁺ stationary-phase promastigotes may be one of the critical survival factors in the detoxification process, which may then influence the metastatic behavior of these parasite populations. Our data further suggest that, once the transformation into an amastigote has been achieved, both M⁺ and M⁻ parasites present similar proportions of dimers and resistance to H₂O₂. At this intracellular stage, the production of NO is mainly under the control of the immune system of the host. We have preliminary results that show a differential pattern of macrophage gene expression when macrophages infected with the M⁻ clone are compared with macrophages infected with the M⁺ clone (S.M. and N.F., unpublished results). We can speculate that the pattern of genes up- or down-regulated by the metastatic *L. (V.) guyanensis* clone optimizes its chances of survival and the eventual dissemination of the parasite, leading to MCL. Thus, different levels of macrophage activation may be induced according to specific characteristics of *Leishmania* parasites on their interaction with the host cell and depending on the genetic background of patients with different disease presentations [35, 36].

In conclusion, the association of the metastatic phenotype with the dimerization of PXN is evident for laboratory clones studied in our model system, which supports the idea that PXN participates in the multifactorial process of metastasis. Furthermore, PXN activity may be exploitable for the early detection of metastasis and, thus, the prevention of metastatic manifestations.

Acknowledgments

We thank Guillaume Esnault, Chantal Desponds, Florence Prevel, and Virginie Dutoit for their technical assistance.

References

1. Weigle K, Saravia NG. Natural history, clinical evolution, and the host-parasite interaction in New World cutaneous leishmaniasis. *Clin Dermatol* **1996**; 14:433–50.
2. Osorio LE, Castillo CM, Ochoa MT. Mucosal leishmaniasis due to *Leishmania (Viannia) panamensis* in Colombia: clinical characteristics. *Am J Trop Med Hyg* **1998**; 59:49–52.
3. Marsden PD. Mucosal leishmaniasis (“espundia” Escomel, 1911). *Trans R Soc Trop Med Hyg* **1986**; 80:859–76.
4. Barral A, Guerreiro J, Bomfi G, Correia D, Barral-Netto M, Carvalho EM. Lymphadenopathy as the first sign of human cutaneous infection by *Leishmania braziliensis*. *Am J Trop Med Hyg* **1995**; 53:256–9.
5. Martinez JE, Alba, Arias L, Escobar MA, Saravia NG. Haemoculture of *Leishmania (Viannia) braziliensis* from two cases of mucosal leishmaniasis: re-examination of haematogenous dissemination. *Trans R Soc Trop Med Hyg* **1992**; 86:392–4.
6. Martinez JE, Travi BL, Valencia AZ, Saravia NG. Metastatic capability of *Leishmania (Viannia) panamensis* and *Leishmania (Viannia) guyanensis* in golden hamsters. *J Parasitol* **1991**; 77:762–8.
7. Travi B, Rey-Ladino J, Saravia NG. Behavior of *Leishmania braziliensis* s.l. in golden hamsters: evolution of the infection under different experimental conditions. *J Parasitol* **1988**; 74:1059–62.
8. Saravia NG, Holguin AF, McMahon-Pratt D, D’Alessandro A. Mucocutaneous leishmaniasis in Colombia: *Leishmania braziliensis* subspecies diversity. *Am J Trop Med Hyg* **1985**; 34:714–20.
9. Bertho AL, Santiago MA, Coutinho SG. An experimental model of the production of metastases in murine cutaneous leishmaniasis. *J Parasitol* **1994**; 80:93–9.
10. Travi BL, Osorio Y, Saravia NG. The inflammatory response promotes cutaneous metastasis in hamsters infected with *Leishmania (Viannia) panamensis*. *J Parasitol* **1996**; 82:454–7.
11. Martinez JE, Valderrama L, Gama V, Leiby DA, Saravia NG. Clonal diversity in the expression and stability of the metastatic capability of *Leishmania guyanensis* in the golden hamster. *J Parasitol* **2000**; 86:792–9.
12. Walker J, Acestor N, Gongora R, et al. Comparative protein profilin identifies elongation factor-1 β and trypanothione peroxidase as factors associated with metastasis in *Leishmania guyanensis*. *Mol Biochem Parasitol* **2006**; 145:254–64.
13. Barr SD, Gedamu L. Cloning and characterization of three differentially expressed peroxidase genes from *Leishmania chagasi*: evidence for an enzymatic detoxification of hydroxyl radicals. *J Biol Chem* **2001**; 276:34279–87.
14. Castro H, Sousa C, Santos M, Cordeiro-da-Silva A, Flohe L, Tomas AM. Complementary antioxidant defense by cytoplasmic and mitochondrial peroxidases in *Leishmania infantum*. *Free Radic Biol Med* **2002**; 33:1552–62.
15. Flohe L, Budde H, Bruns K, et al. Trypanothione peroxidase of *Leishmania donovani*: molecular cloning, heterologous expression, specificity, and catalytic mechanism. *Arch Biochem Biophys* **2002**; 397:324–35.
16. Levick MP, Tetaud E, Fairlamb AH, Blackwell JM. Identification and characterization of a functional peroxidase from *Leishmania major*. *Mol Biochem Parasitol* **1998**; 96:125–37.
17. Nogoceke E, Gommel DU, Kiess M, Kalisz HM, Flohe L. A unique cascade of oxidoreductases catalyses trypanothione-mediated peroxide metabolism in *Crithidia fasciculata*. *Biol Chem* **1997**; 378:827–36.
18. Tetaud E, Giroud C, Prescott AR, et al. Molecular characterization of mitochondrial and cytosolic trypanothione-dependent trypanothione peroxidases in *Trypanosoma brucei*. *Mol Biochem Parasitol* **2001**; 116:171–83.
19. Wilkinson SR, Temperton NJ, Mondragon A, Kelly JM. Distinct mitochondrial and cytosolic enzymes mediate trypanothione-dependent peroxide metabolism in *Trypanosoma cruzi*. *J Biol Chem* **2000**; 275:8220–5.
20. Wood ZA, Schroder E, Robin Harris J, Poole LB. Structure, mechanism and regulation of peroxiredoxins. *Trends Biochem Sci* **2003**; 28:32–40.
21. Green SJ, Crawford RM, Hockmeyer JT, Meltzer MS, Nacy CA. *Leishmania major* amastigotes initiate the L-arginine-dependent killing mechanism in IFN- γ -stimulated macrophages by induction of tumor necrosis factor- α . *J Immunol* **1990**; 145:4290–7.
22. Liew FY, Millott S, Parkinson C, Palmer RM, Moncada S. Macrophage killing of *Leishmania* parasite in vivo is mediated by nitric oxide from L-arginine. *J Immunol* **1990**; 144:4794–7.
23. Koo KH, Lee S, Jeong SY, et al. Regulation of thioredoxin peroxidase activity by C-terminal truncation. *Arch Biochem Biophys* **2002**; 397:312–8.
24. McGonigle S, Dalton JP, James ER. Peroxidoxins: a new antioxidant family. *Parasitol Today* **1998**; 14:139–45.
25. Sacks DL, Perkins PV. Identification of an infective stage of *Leishmania* promastigotes. *Science* **1984**; 223:1417–9.
26. Goyal N, Roy U, Rastogi AK. Relative resistance of promastigotes of a virulent and an avirulent strain of *Leishmania donovani* to hydrogen peroxide. *Free Radic Biol Med* **1996**; 21:683–9.
27. Corradin SB, Mauel J. Phagocytosis of *Leishmania* enhances macrophage activation by IFN- γ and lipopolysaccharide. *J Immunol* **1991**; 146:279–85.
28. Corradin SB, Buchmuller-Rouiller Y, Mauel J. Phagocytosis enhances murine macrophage activation by interferon- γ and tumor necrosis factor- α . *Eur J Immunol* **1991**; 21:2553–8.
29. Hofmann B, Hecht HJ, Flohe L. Peroxiredoxins. *Biol Chem* **2002**; 383:347–64.
30. Zarley JH, Britigan BE, Wilson ME. Hydrogen peroxide-mediated toxicity for *Leishmania donovani chagasi* promastigotes: role of hydroxyl radical and protection by heat shock. *J Clin Invest* **1991**; 88:1511–21.
31. Wagner E, Luche S, Penna L, et al. A method for detection of over-oxidation of cysteines: peroxiredoxins are oxidized in vivo at the active-site cysteine during oxidative stress. *Biochem J* **2002**; 366:777–85.
32. Fratelli M, Demol H, Puype M, et al. Identification by redox proteomics of glutathionylated proteins in oxidatively stressed human T lymphocytes. *Proc Natl Acad Sci USA* **2002**; 99:3505–10.
33. Miller MA, McGowan SE, Gantt KR, et al. Inducible resistance to oxidant stress in the protozoan *Leishmania chagasi*. *J Biol Chem* **2000**; 275:33883–9.
34. Jang HH, Lee KO, Chi YH, et al. Two enzymes in one; two yeast peroxiredoxins display oxidative stress-dependent switching from a peroxidase to a molecular chaperone function. *Cell* **2004**; 117:625–35.
35. Nashleas M, Kanaly S, Scott P. Control of *Leishmania major* infection in mice lacking TNF receptors. *J Immunol* **1998**; 160:5506–13.
36. Cabrera M, Shaw MA, Sharples C, et al. Polymorphism in tumor necrosis factor genes associated with mucocutaneous leishmaniasis. *J Exp Med* **1995**; 182:1259–64.
37. Solioz N, BluM-Tirouvanziam U, Jacquet R, et al. The protective capacities of histone H1 against experimental murine cutaneous leishmaniasis. *Vaccine* **1999**; 18:850–9.
38. Puentes F, Diaz D, Hoya RD, et al. Cultivation and characterization of stable *Leishmania guyanensis* complex axenic amastigotes derived from infected U937 cells. *Am J Trop Med Hyg* **2000**; 63:102–10.
39. Flohe L, Steinert P, Hecht HJ, Hofmann B. Trypanothione and trypanothione peroxidase. *Methods Enzymol* **2002**; 347:244–58.
40. Corradin S, Mauel J, Ransijn A, Sturzingger C, Vergeres G. Down-regulation of MARCKS-related protein (MRP) in macrophages infected with *Leishmania*. *J Biol Chem* **1999**; 274:16782–7.